

CHAPTER V

RESULTS AND DISCUSSIONS

This chapter was conducted in order to investigate the characteristic and catalytic properties of spherical silica and alumina-silica composites-supported cobalt catalysts for carbon dioxide hydrogenation reaction. This chapter is divided into two sections. The first section describes the preparation and characterization of spherical silica and alumina-silica composites supports. The second section shows characteristics and catalytic activity of spherical silica and alumina-silica composites supported cobalt catalysts.

5.1 Support preparation and characterization

This section described the preparation and characterization of spherical silica and alumina-silica composite supports by deposition of Al_2O_3 particles on the spherical silica particle (SSP) surface using hydrolysis of aluminium isopropoxide to obtain AISSP.

5.1.1 Preparation of spherical silica particle (SSP)

Scanning electron microscopy (SEM) characterization was used to investigate the morphology of spherical silica support. Figure 5.1 shows images of spherical particles, with an average size of about $0.5\ \mu\text{m}$.



Figure 5.1 The SEM images of the spherical silica particles.

The specific surface area, pore size and pore volume of spherical silica particles were measured by nitrogen physisorption technique. The results are summarized in Table 5.1.

Table 5.1 BET surface area, pore volume and pore diameter of spherical silica particles

Sample	Surface area (m ² /g)	Pore volume (cm ³ /g)	Pore diameter (nm)
SSP550	927	0.7508	2.18

5.1.2 Preparation and characterization of alumina-spherical silica particles composites supports (AISSP)

This section described the characterization of spherical silica and alumina-silica composite supports by deposition of Al_2O_3 particles on the spherical silica particle (SSP). The structure and crystallinity of the alumina-silica composite supports (AISSP) were measured by BET surface area, X-ray diffraction, scanning electron microscopy (SEM), energy dispersive X-ray spectroscopy (EDX) and transmission electron microscope (TEM) were used to study the morphology of the alumina-silica composites supports. The thermal properties of the alumina-silica composites supports were characterized by differential thermal analysis and thermogravimetric (DTA/TG).

5.1.2.1 Differential thermal analysis and thermogravimetric (DTA/TG)

The thermal property was characterized by thermogravimetric and differential thermal analysis (TG-DTA). Figure 5.2 shows the endothermic peaks of differential thermal analysis (DTA) curve of AISSP below 600°C . The weight loss corresponding to dehydration was observed in the thermal analysis TG curve. The noticeable exothermal peak at 992°C was related to the XRD patterns as mentioned after. The DTA curve indicated the exothermic peak that was due to the phase transformation of amorphous to γ -alumina at 992°C . The TG curve had shown a largest weight loss about 12.5% in AISSP.

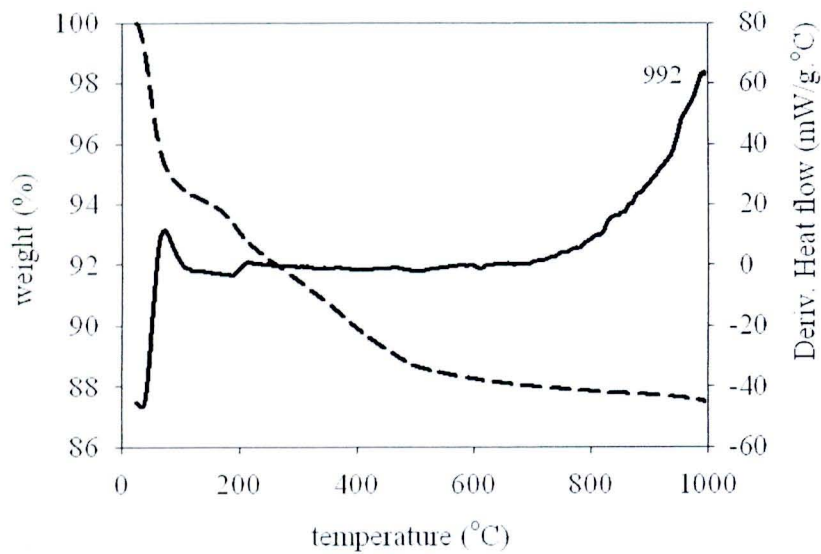


Figure 5.2 DTA/TG curve of the AlSSP (1:3) composites.

5.1.2.2 X-Ray Diffraction

Bulk crystal structure and chemical phase composition of a crystalline material having crystal domain of greater than 3-5 nm can be determined by X-ray diffraction. The measurements were carried out at the diffraction angles (2θ) between 20° and 80° .

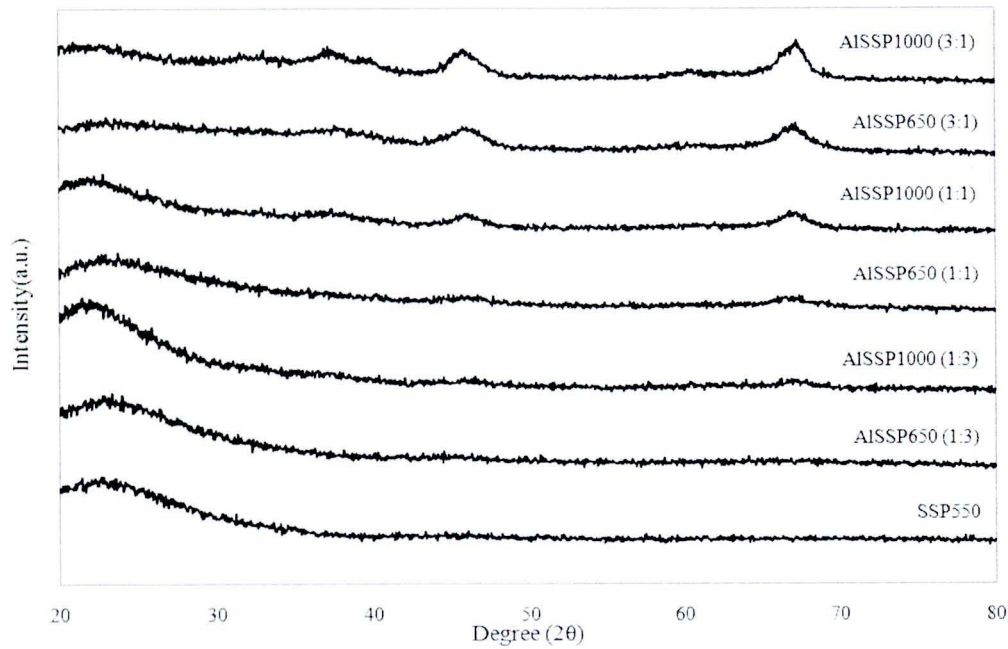


Figure 5.3 XRD patterns of spherical silica and alumina-silica composite supports.

XRD patterns of spherical silica (SSP) and alumina-silica composite supports (AISSP) before impregnation with the cobalt metal at various calcination temperatures for 2 h and various compositions between alumina and silica are shown in Figure 5.3. After calcined at 550°C for 2 h, the XRD patterns of SSP550 exhibited only amorphous silica. At 650 and 1000°C, the slight diffraction peak of Al_2O_3 crystallite can be observed at 33.08, 37.2, 45.84, and 67.28°. This demonstrates that Al_2O_3 had a small significant crystalline size of γ -alumina. Therefore, thermal stability of γ -alumina can be enhanced by adding spherical silica. At various composition between alumina and silica, AISSP1000 (3:1) had a highest large γ -alumina crystallite size compared with AISSP1000 (1:3).

5.1.2.3 Nitrogen physisorption

The BET surface area, pore volume and average pore diameter analysis of alumina-silica composite supports (AISSP) at various calcination temperatures for 2 h and various compositions between alumina and silica are listed in Table 5.2, which are measured by nitrogen physisorption technique.

From the result, it can be observed that the surface areas of all AISSP supports were less than the pure spherical silica particle. This was in accordance with the larger pore sizes of AISSP supports than those of pure spherical silica support. This is probably due to the increase of alumina amount in the spherical silica particle. At various calcination temperatures, AISSP650 (1:3) exhibited the best possible BET surface area of 769 m^2/g . Moreover, the BET surface area and pore volume dramatically decreased to 23 m^2/g for AISSP1000 (1:3). This is probably due to the sintering effect. However, BET surface area increased with alumina loading from 23 m^2/g of AISSP1000 (1:3) to 76 and 134 m^2/g of AISSP1000 (1:1) and AISSP1000 (3:1), respectively as shown in Table 5.2. This can be attributed to grain growth from phase transformation of amorphous to γ -alumina and the particles sintering. The smaller γ -alumina crystallites grow into bigger γ -alumina crystallites through the phase transformation as the results from Figure 5.3, leading to the decrease of the voids among γ -alumina crystallites.

Table 5.2 BET Surface areas, pore volume and pore diameter of alumina-spherical silica particle composites.

Samples	Surface area (m ² /g)	Pore Volume (cm ³ /g)	Pore Diameter (nm)
AlSSP650 (1:3)	769	0.6247	2.56
AlSSP1000 (1:3)	23	0.0452	6.92
AlSSP650 (1:1)	529	0.5282	3.69
AlSSP1000 (1:1)	76	0.2362	9.09
AlSSP650 (3:1)	443	0.7278	5.62
AlSSP1000 (3:1)	134	0.4762	9.35

5.1.2.4 Scanning electron microscopy (SEM) and energy dispersive X-ray spectroscopy (EDX)

Scanning electron microscopy (SEM) and energy dispersive X-ray spectroscopy (EDX) was also conducted in order to study surface texture, morphology and elemental distribution of the materials, respectively. In the backscattering scanning mode, the electron beam focused on the sample is scanned by a set of deflection coils. Backscattered electrons or secondary electrons emitted from the sample are detected. The typical SEM micrograph, EDX mapping and a typical spectrum from EDX analysis for AlSSP650 (3:1) was illustrated in Figure 5.4 and Figure 5.5. The external surface of support granule was shown in this figure and light or white patches on the support granule surface representing high concentration of silica, alumina and oxygen distribution on the surface. It indicated that the alumina distribution on the spherical silica surface is uniform.

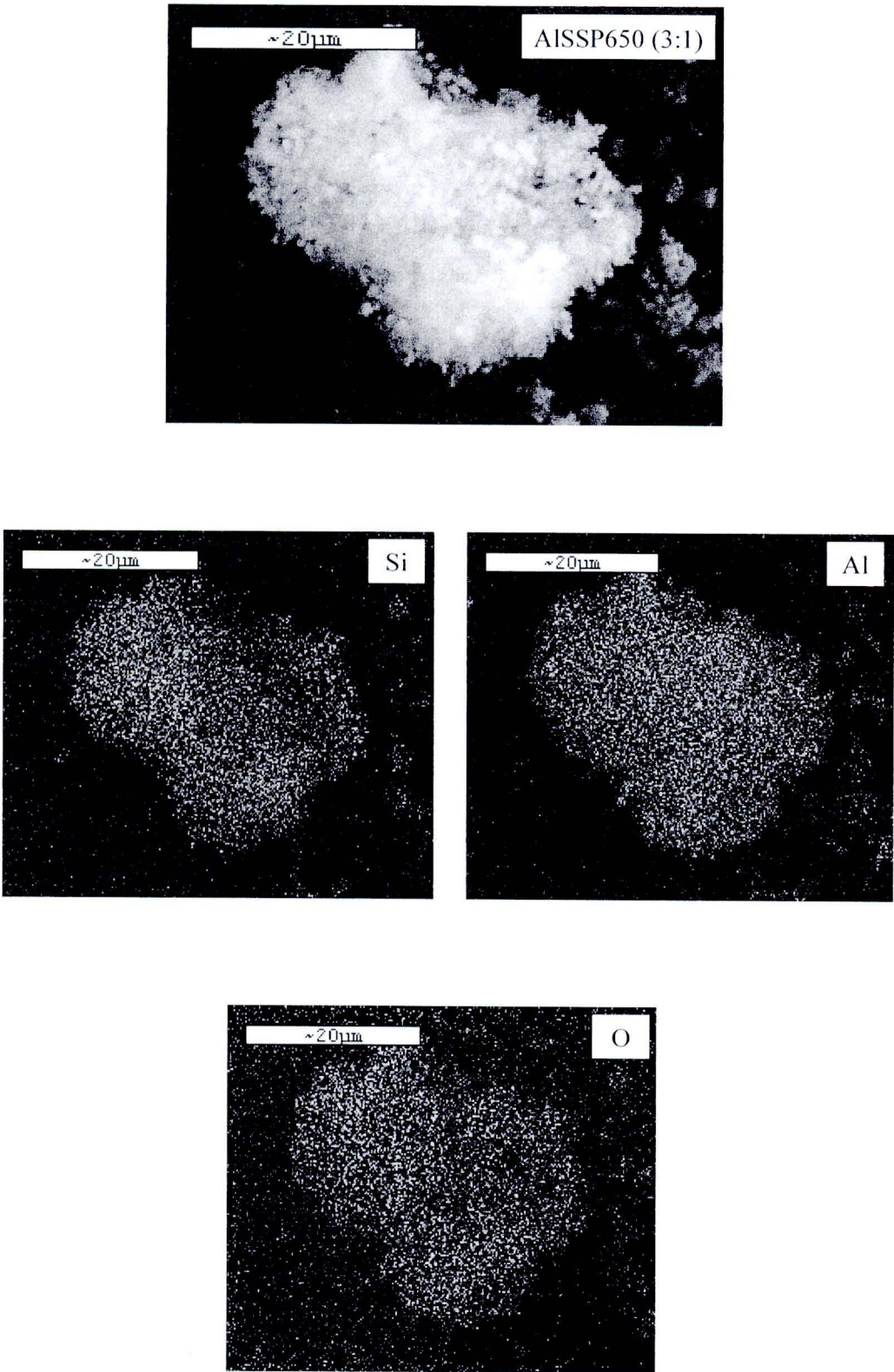
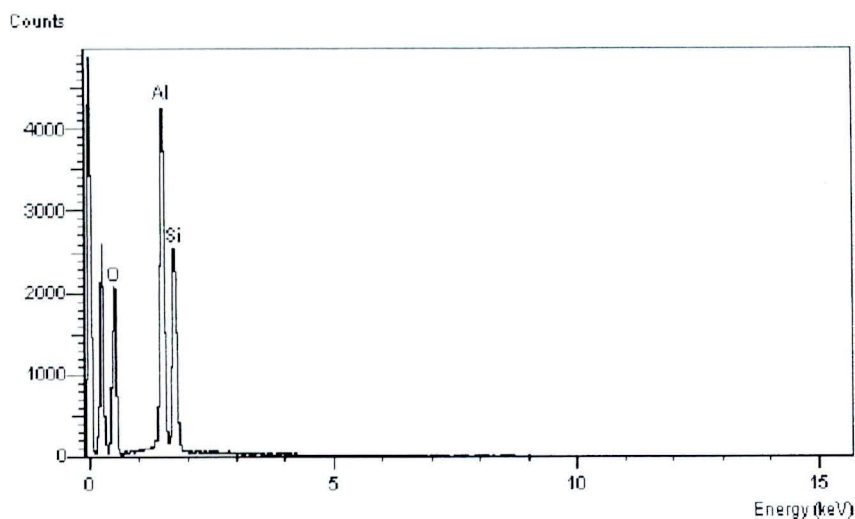


Figure 5.4 SEM micrograph and EDX mapping of AlSSP650 (3:1) composites.



Element	Element (%)	Atomic (%)
Si	17.42	12.67
Al	25.87	20.01
O	56.71	67.32

Figure 5.5 A typical spectrum of the AlSSP650 (3:1) composites from EDX analysis.

5.1.2.5 Transmission electron microscope (TEM)

In order to determine the dispersion of alumina on the spherical silica employed, the high resolution TEM was used. The TEM micrographs for alumina-silica composites support, AlSSP650 (1:3) is shown in Figure 5.6. As seen in this figure, the dark spots representing the alumina on the spherical silica was well dispersed. TEM image was found to be similar with the results from SEM/ EDX.

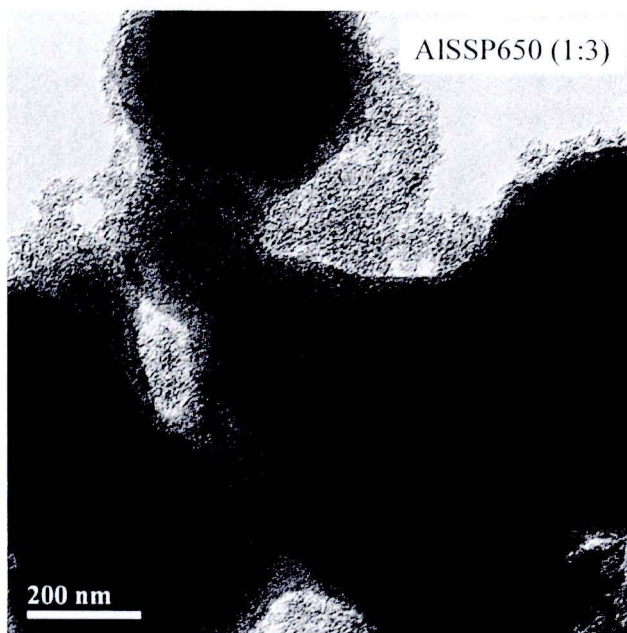


Figure 5.6 TEM micrographs of the AlSSP650 (1:3) composites.

5.2 Preparation and characterization of spherical silica (SSP) and alumina-spherical silica composites (AlSSP) supported cobalt catalyst.

This section presented the characterization of silica and alumina-silica composites supported cobalt catalyst by incipient wetness impregnation of cobalt (II) nitrate hexahydrate. The various analytical techniques had been performed including BET surface area, X-ray diffraction, scanning electron microscopy (SEM), energy dispersive X-ray spectroscopy (EDX), transmission electron microscope (TEM), temperature programmed reduction (TPR), CO chemisorptions and CO₂ hydrogenation reaction performance.

5.2.1 X-ray diffraction

The phase identification was carried out on the basis of data from X-ray diffraction. A 20% wt of cobalt was impregnated onto spherical silica (SSP) and alumina-silica composite supports (AlSSP). After calcination in air at 500°C for 4 h, the XRD patterns for the calcined Co catalysts for all supports are shown in Figure 5.7. The XRD peaks of Co₃O₄ were observed at 31°, 37°, 45°, 59°, and 65°

[Jakrapan, 2009]. XRD peaks of $\gamma\text{-Al}_2\text{O}_3$ were not observed due to high intensity of the Co_3O_4 peaks.

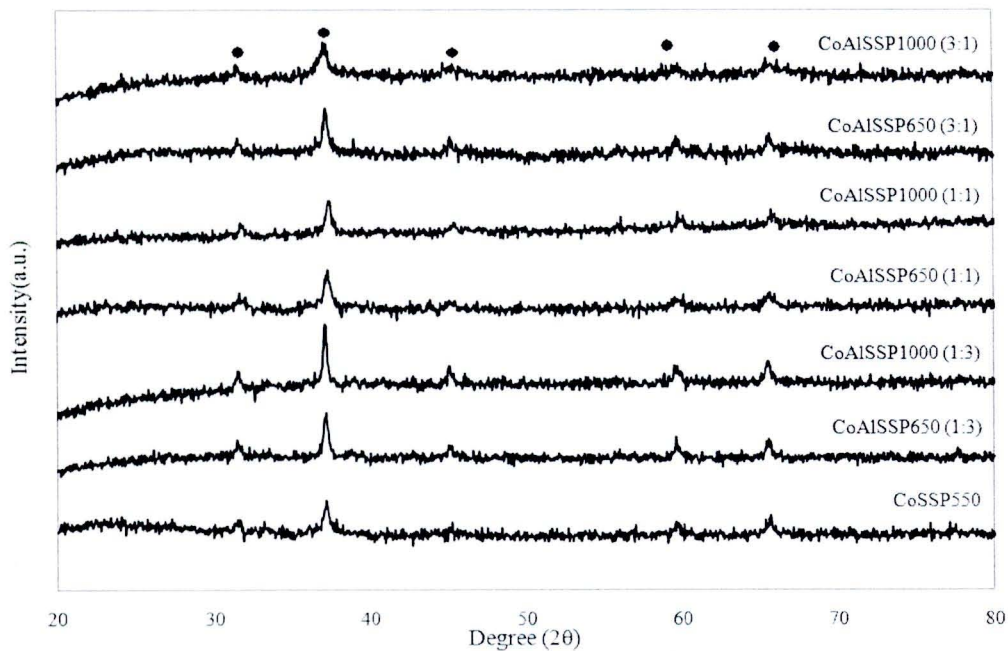


Figure 5.7 XRD patterns of silica and alumina-silica composites supported cobalt catalysts.

5.2.2 Nitrogen physisorption

The BET surface areas, pore volume and average pore diameter analysis of cobalt impregnated onto SSP and AlSSP after calcination for 6 hours at 500°C were measured by nitrogen physisorption technique as shown in Table 5.3. The surface areas of CoSSP and all CoAlSSP were less than the corresponding supports. This was in accordance with the smaller pore sizes of CoSSP550, CoAlSSP650 and CoAlSSP1000 catalysts than those of pure support particles.

Table 5.3 BET Surface areas, pore volume and pore diameter of silica and alumina-silica composites-supported cobalt catalysts.

Samples	Surface area (m ² /g)	Pore Volume (cm ³ /g)	Pore Diameter (nm)
CoSSP550	631	0.4578	2.46
CoAlSSP650 (1:3)	490	0.2528	2.36
CoAlSSP1000 (1:3)	25	0.0405	5.16
CoAlSSP650 (1:1)	380	0.2818	3.66
CoAlSSP1000 (1:1)	63	0.1715	8.15
CoAlSSP650 (3:1)	244	0.2998	4.69
CoAlSSP1000 (3:1)	102	0.2979	8.81

5.2.3 Scanning electron microscopy (SEM) and energy dispersive X-ray spectroscopy (EDX)

Scanning electron microscopy (SEM) and energy dispersive X-ray spectroscopy (EDX) were also conducted in order to study the morphologies and elemental distribution of the samples, respectively. The SEM micrographs and EDX mapping for spherical silica supported cobalt catalyst; CoSSP550 was illustrated in Figure 5.9 and Figure 5.10. The external surface of catalyst granule was shown. In all figures, the light or white patches on the catalyst granule surface represent high concentration of cobalt oxides on the surface. It can be seen that cobalt is well distributed on the external surface.

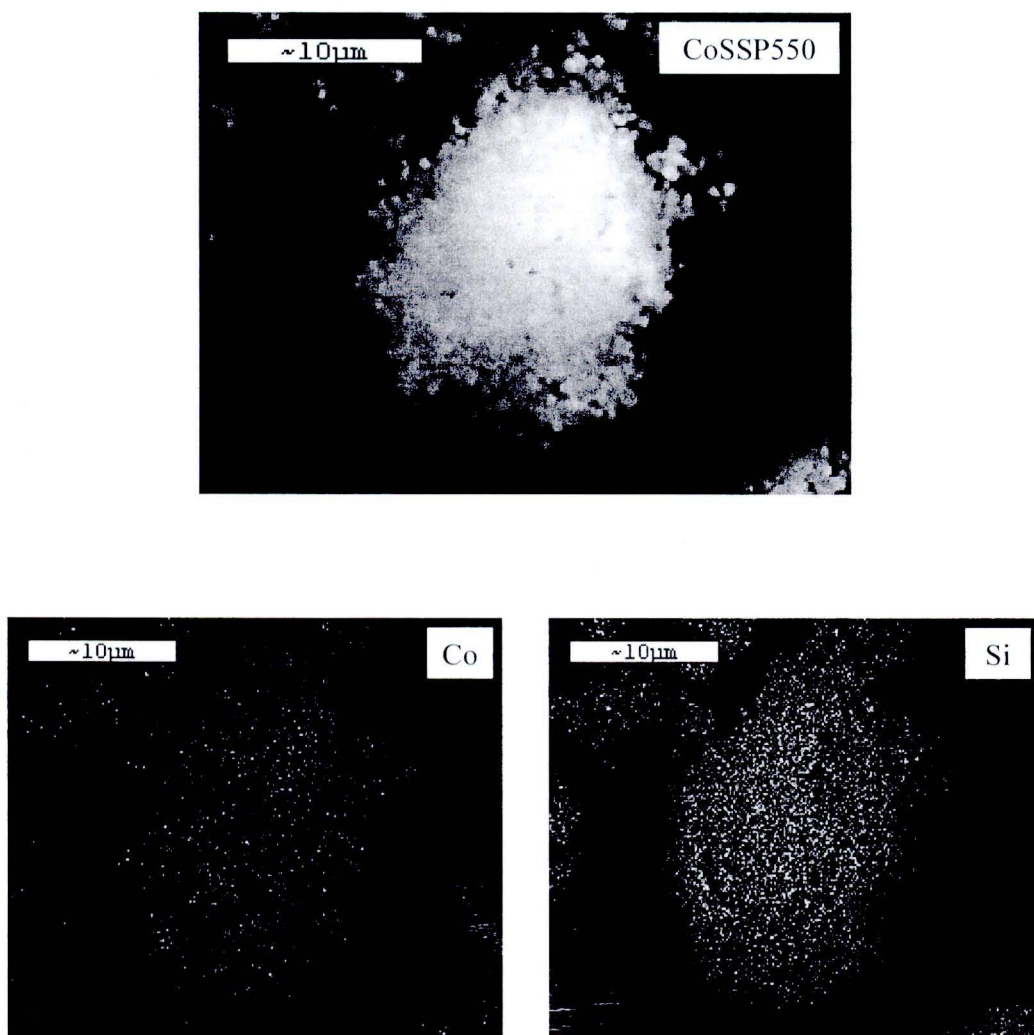
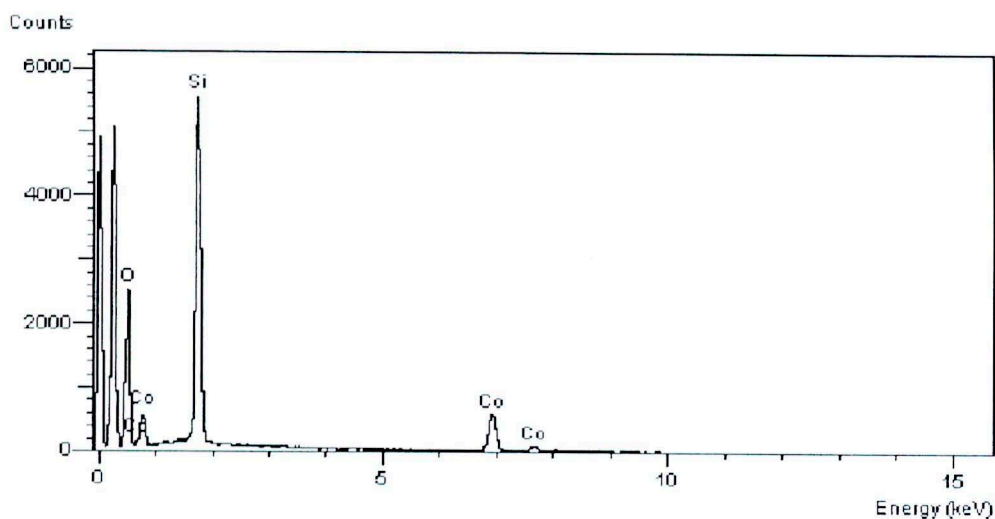


Figure 5.8 SEM micrograph and EDX mapping of CoSSP550 catalyst.



Element	Element (%)	Atomic (%)
Si	30.37	22.88
Co	15.55	5.58
O	54.08	71.53

Figure 5.9 A typical spectrum of the CoSSP550 catalyst from EDX analysis.

Figures 5.10- 5.15 are shown the morphologies and elemental distribution of the samples. Figure 5.16 presents a typical spectrum and element quantity of CoAlSSP650 (3:1) surface from EDX analysis. It can be seen that the cobalt oxide species was well dispersed on alumina-silica composite supports.

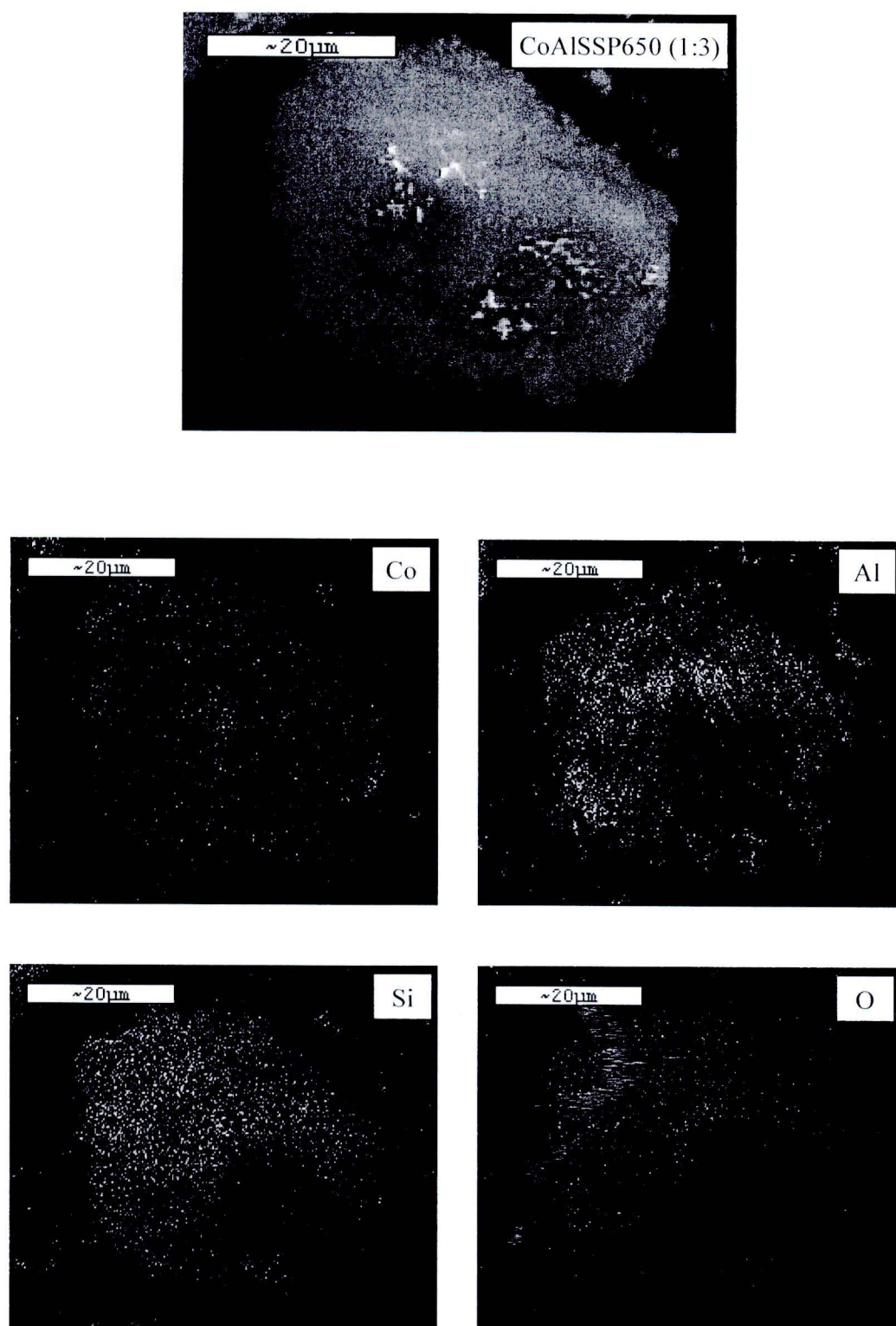


Figure 5.10 SEM micrograph and EDX mapping of CoAlSSP650 (1:3) catalyst.

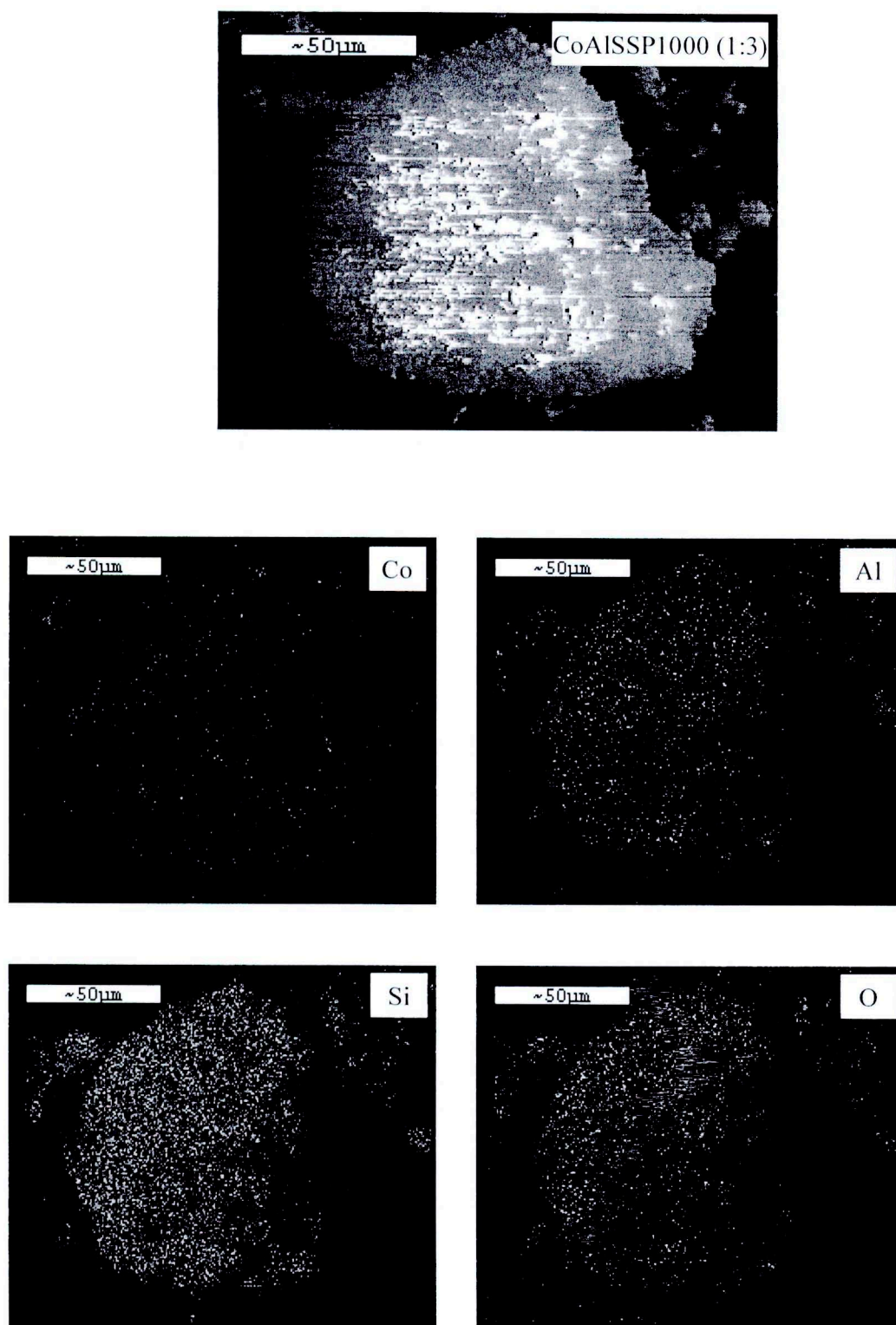


Figure 5.11 SEM micrograph and EDX mapping of CoAlSSP1000 (1:3) catalyst.

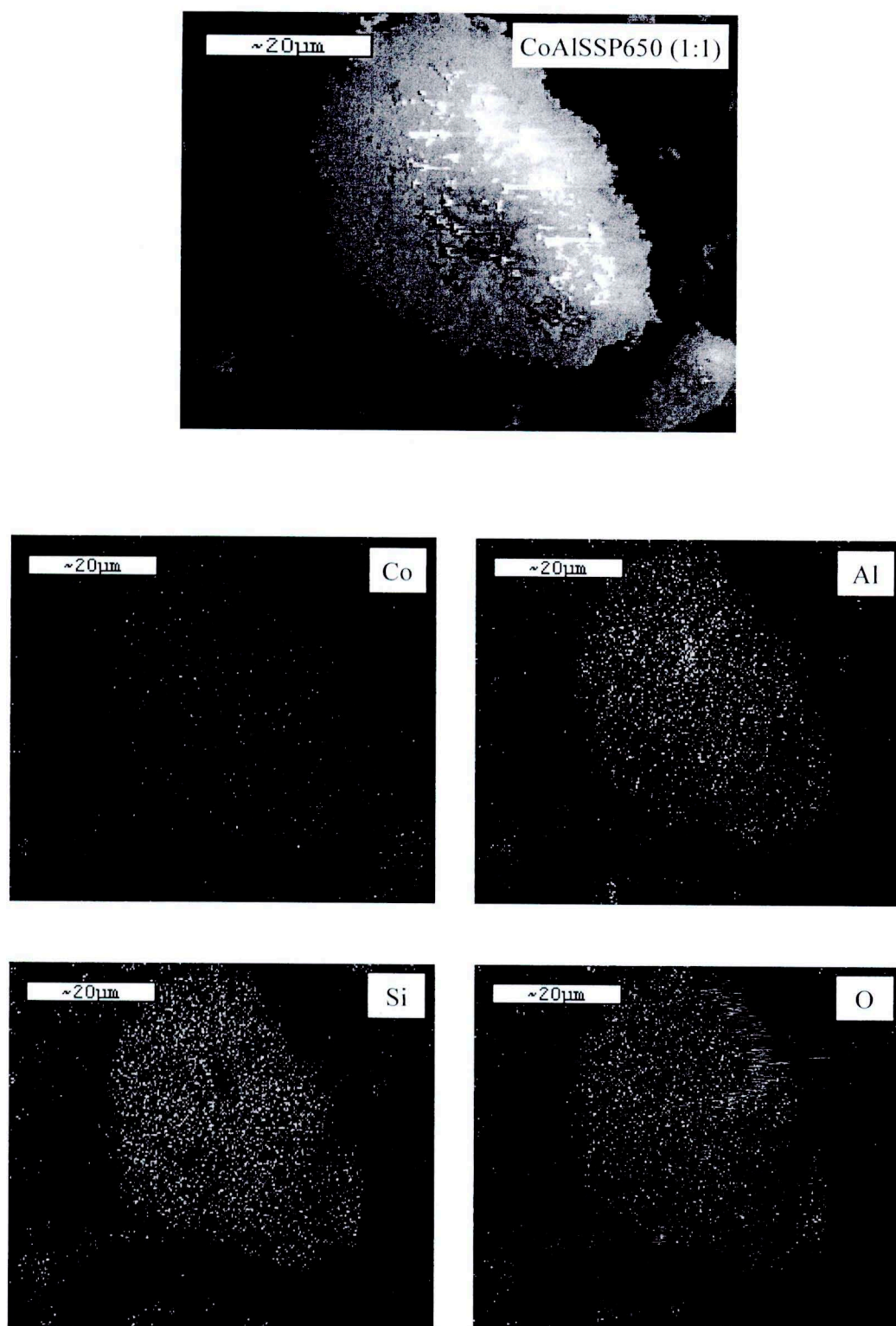


Figure 5.12 SEM micrograph and EDX mapping of CoAlSSP650 (1:1) catalyst.

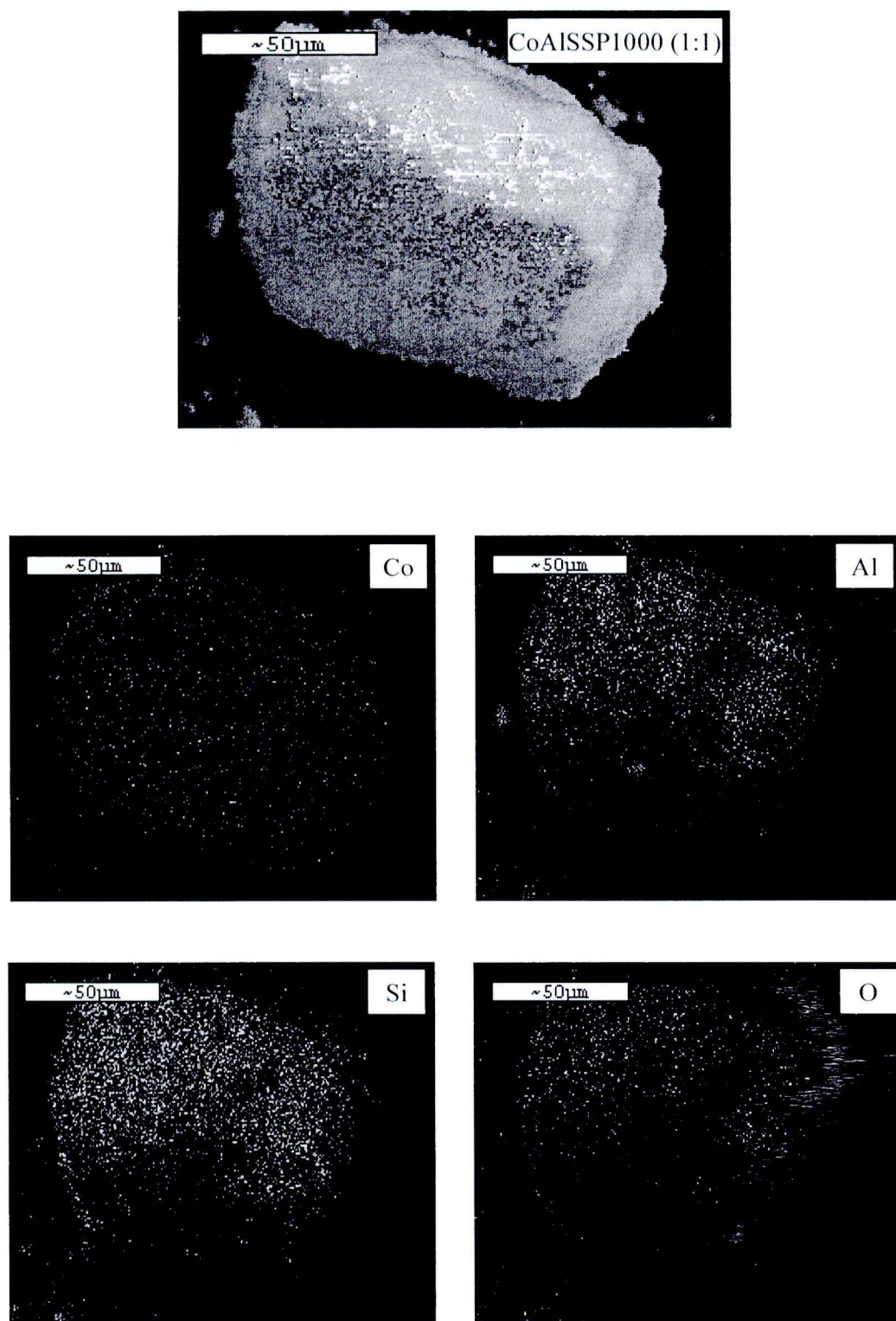


Figure 5.13 SEM micrograph and EDX mapping of CoAlSSP1000 (1:1) catalyst.

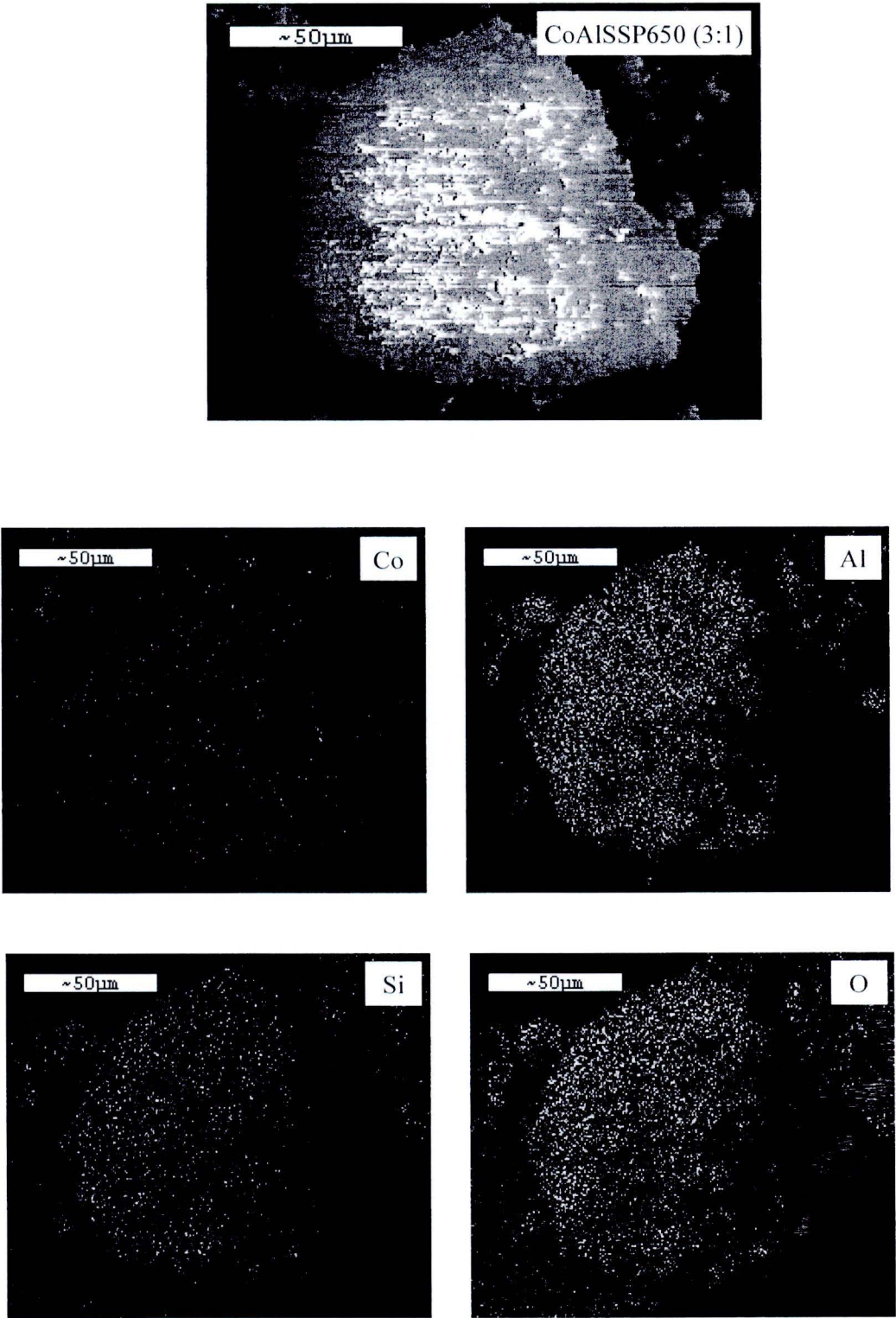


Figure 5.14 SEM micrograph and EDX mapping of CoAlSSP650 (3:1) catalyst.

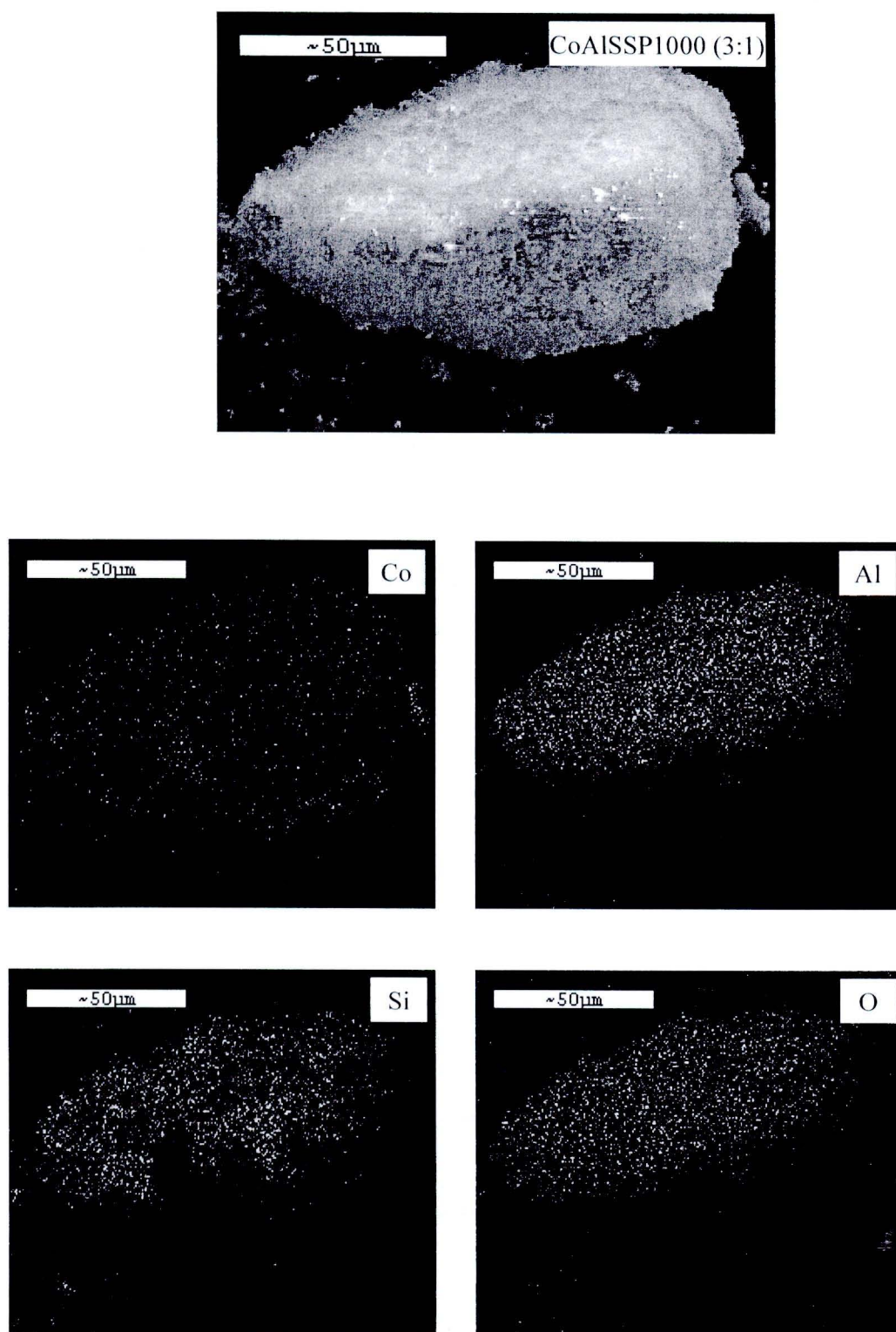
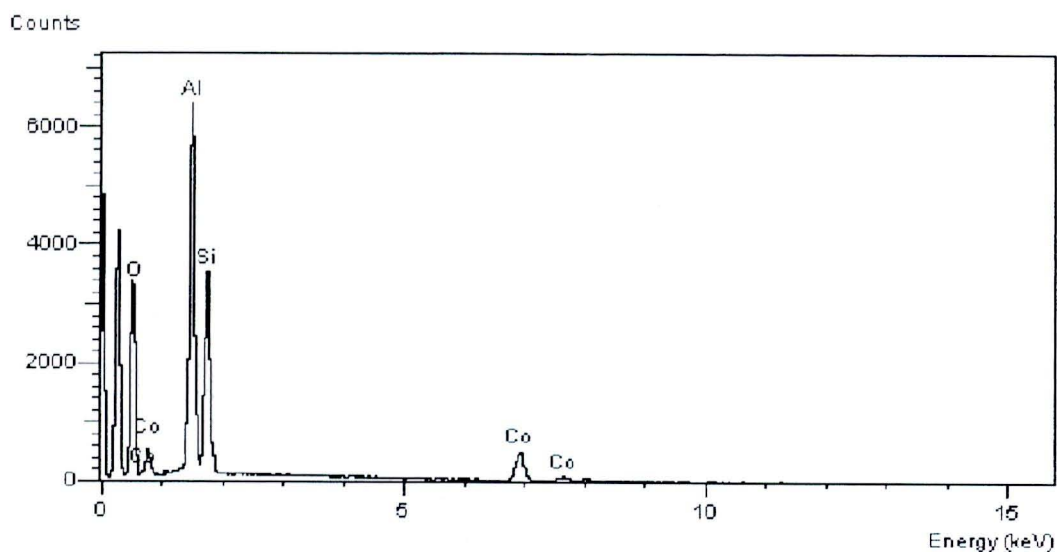


Figure 5.15 SEM micrograph and EDX mapping of CoAlSSP1000 (3:1) catalyst.

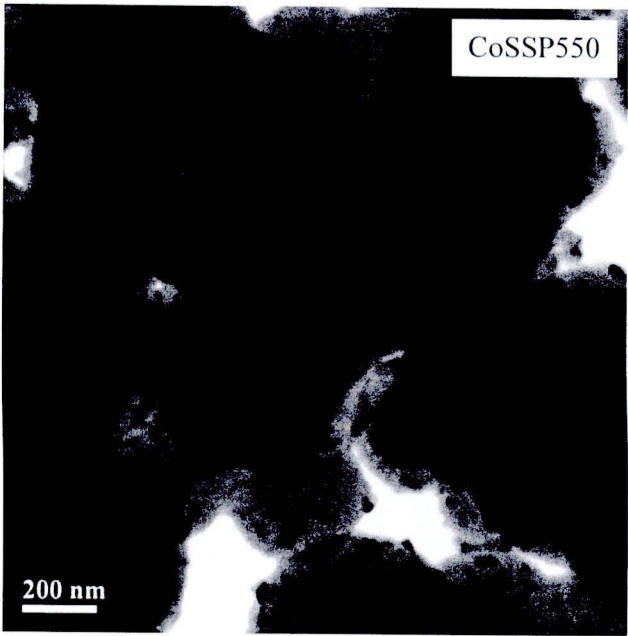


Element	Element (%)	Atomic (%)
Si	16.62	12.43
Al	24.61	19.16
Co	9.16	12.43
O	49.61	65.14

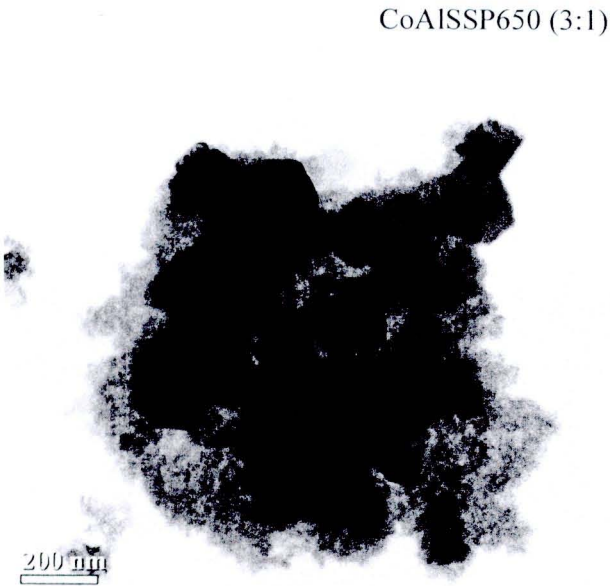
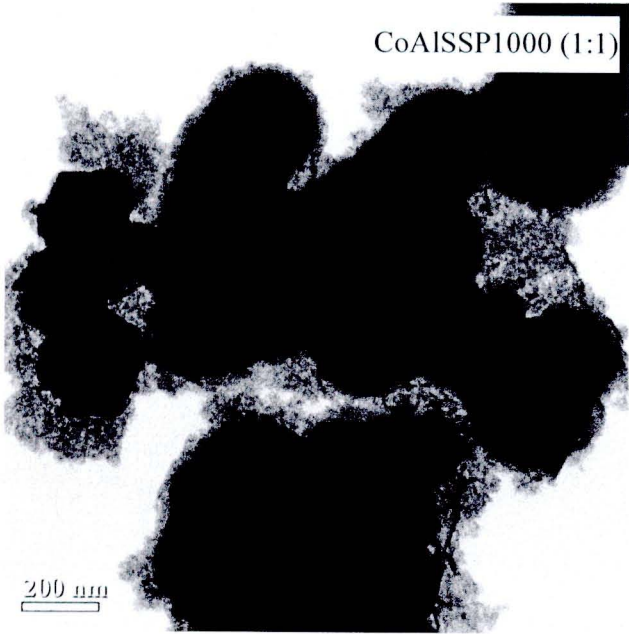
Figure 5.16 A typical spectrum of the CoAlSSP650 (3:1) catalyst from EDX analysis.

5.2.4 Transmission electron microscope (TEM)

In order to determine the dispersion and crystallite size of cobalt oxides species dispersed on the spherical silica support and alumina-silica composites supports, TEM of samples are shown in Figure 5.17. Apparently, the cobalt oxide species on the spherical silica and alumina-silica composites supports were well dispersed.







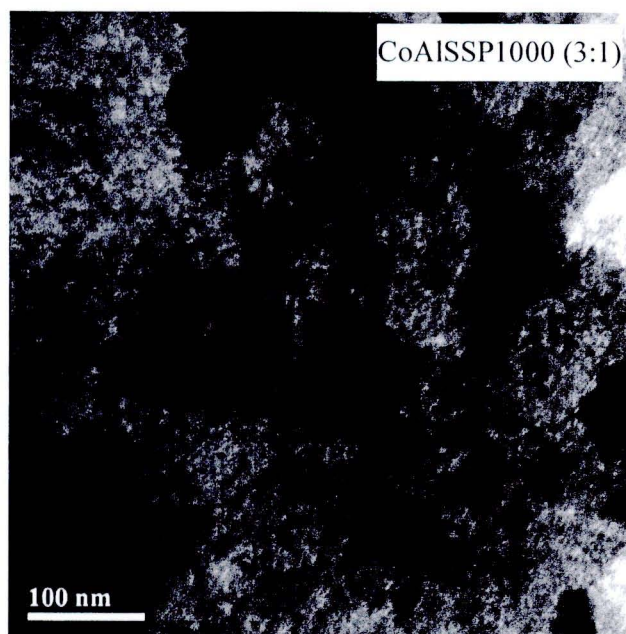


Figure 5.17 TEM micrograph for the silica and alumina-silica composites supported cobalt catalysts.

5.2.5 Temperature Programmed Reduction (TPR)

As mentioned, TPR was performed in order to determine the reduction behaviors of cobalt oxides species on various supports. The TPR profiles for cobalt supported on spherical silica and alumina-silica composites supports were shown in Figure 5.18. Based on these profiles, the reducibilities for each catalyst are also given in Table 5.4. Reduction was observed for all catalysts, which can be assigned to the overlap of two peak reduction. The first peak has been ascribed the reduction of Co_3O_4 to CoO , followed by the second peak which corresponds to the reduction of CoO to Co^0 [Saib et al., 2002]. Besides reduction behaviors obtained from TPR results, reducibility of the catalysts can be measured based on the peak area below TPR curve. From the silica supported cobalt catalyst result, the TPR peak located at 200 to 800°C. However, this reduction peak was slightly shifted to higher temperatures with increasing the amount of alumina present in the composite supports. In addition, increased amounts of alumina caused in the decreased

reducibility due to strong support interaction between cobalt oxide species and the support [Marie et al., 2009; Sun et al., 2010].

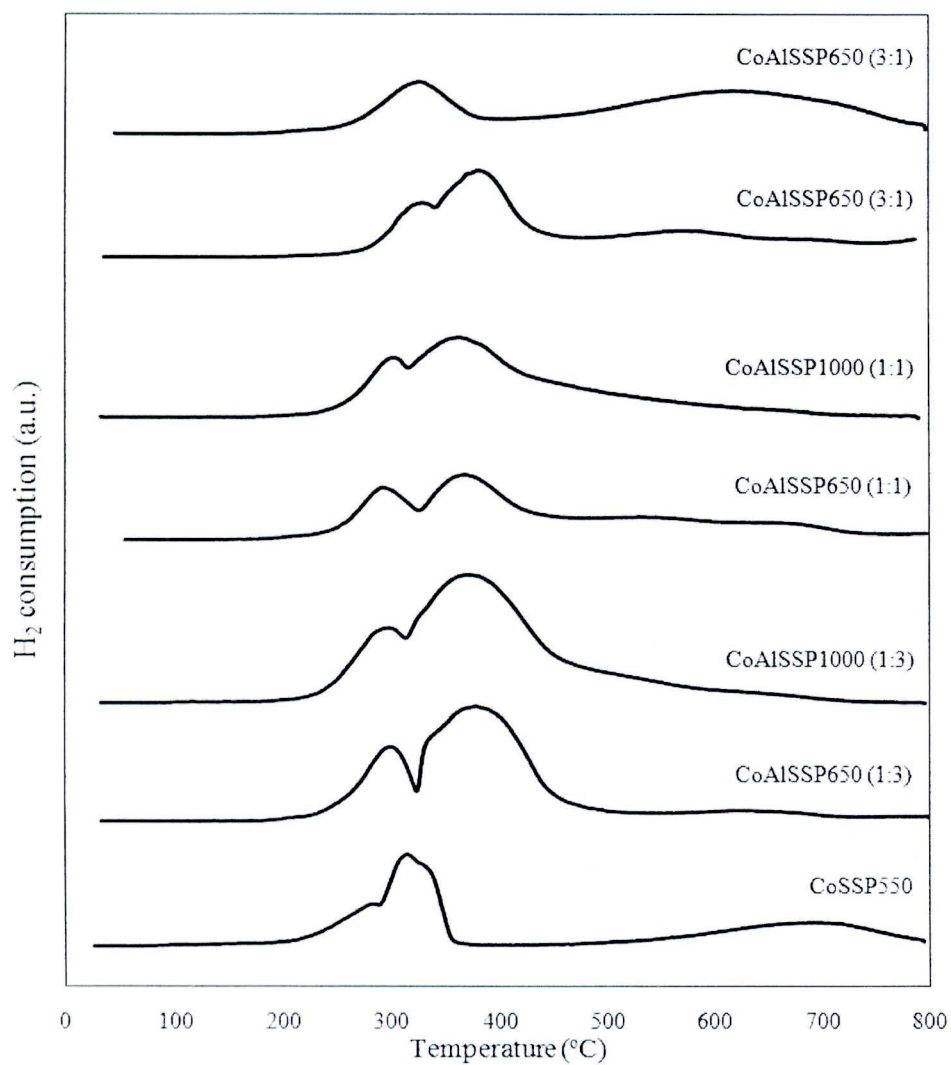


Figure 5.18 TPR patterns of the silica and alumina-silica composites supported cobalt catalysts.

Table 5.4 H₂ consumption from TRP profiles of silica and alumina-silica composites-supported cobalt catalysts.

Samples	Total H ₂ consumption ($\mu\text{mol H}_2/\text{g.cat}$)	Reducibility (%)
CoSSP550	1538	33.98
CoAlSSP650 (1:3)	1948	43.04
CoAlSSP1000 (1:3)	2124	46.95
CoAlSSP650 (1:1)	1324	29.25
CoAlSSP1000 (1:1)	953	21.07
CoAlSSP650 (3:1)	1523	33.66
CoAlSSP1000 (3:1)	1308	28.90

5.2.6 CO-chemisorptions

Active site of catalysts can be determined by calculation from amount of carbon monoxide adsorption on catalysts. The calculation of active site for all catalysts is shown in Appendix B. Absorbed amount of carbon monoxide is directly proportional to the active site. The higher absorbed amount of carbon monoxide means the higher active site. The characterization results of CO chemisorptions for the catalyst samples are illustrated in Table 5.5.

Table 5.5 Amount of carbon monoxide adsorbed on silica and alumina-silica composites-supported cobalt catalysts.

Sample	Active site molecule ^{10¹⁸} per g.cat	Total CO chemisorption μmol CO /g. cat	% Dispersion of Cobalt
CoSSP550	12.8	21.27	0.63
CoAlSSP650 (1:3)	12.71	21.11	0.62
CoAlSSP1000(1:3)	11.24	18.66	0.55
CoAlSSP650 (1:1)	8.45	14.04	0.41
CoAlSSP1000 (1:1)	7.33	12.17	0.36
CoAlSSP650 (3:1)	6.14	10.2	0.30
CoAlSSP1000 (3:1)	9.7	16.11	0.47

From the result, the amounts of CO adsorbed were 12.8 ($\times 10^{18}$ mol g cat⁻¹) for spherical silica supported catalyst and in the range of 6.14 to 12.71 ($\times 10^{18}$ mol g cat⁻¹) for alumina-silica composited supported catalysts. It revealed that the number of reduced cobalt metal surface atoms slightly decreased with increasing the amount of alumina present in the composites supports. Since only Co metal has significant activity for CO hydrogenation, these results were consistent with CO chemisorption results.

5.2.7 Catalytic activity for CO₂-hydrogenation over spherical silica and alumina-silica composites supported cobalt catalyst.

In order to determine the catalytic behaviors of the cobalt supported on spherical silica and alumina-silica composites supports, CO₂ hydrogenation (H₂/CO₂ = 10.36/1) under methanation condition was performed to determine the overall activity and product selectivity of the samples. Before reaction, the catalysts were reduced in-situ in H₂ flow 50 ml/min at 350°C for 3 h in order to obtain metallic phase cobalt. Hydrogenation of CO₂ was carried out at 220°C. A flow rate of H₂/CO₂/Ar = 19.3344/1.8656/8.8 cm³/min in a fixed-bed flow reactor was used. The resulted reaction test is shown in Table 5.6 and Figure 5.19.

Table 5.6 Activity and product selectivity of spherical silica and alumina-silica composites supported cobalt catalysts.

Samples	CO ₂ Conversion ^a		Selectivity ^c		Rate ^c
	(%)		(%)		(x10 ² gCH ₄ / gcat. h)
	Initial ^b	SS ^c	CH ₄	CO	SS ^c
CoSSP550	18.84	19.97	91.77	8.23	10.85
CoAlSSP650 (1:3)	33.97	19.98	91.26	8.74	10.09
CoAlSSP1000 (1:3)	35.85	26.12	94.02	5.96	14.21
CoAlSSP650 (1:1)	29.93	24.26	93.30	6.69	14.35
CoAlSSP1000 (1:1)	16.99	11.78	85.20	14.80	6.30
CoAlSSP650(3:1)	29.94	21.16	91.73	8.27	11.15
CoAlSSP1000 (3:1)	17.38	18.08	90.83	9.17	10.85

^a CO₂ hydrogenation was carried out at 220°C, 1 atm, H₂/CO₂/Ar = 19.3344/1.8656/8.8, and F/W = 18L/ gcat. h.

^b After 5 min of reaction.

^c After 4 h of reaction.

Table 5.6 shows the results from hydrogenation of CO_2 that was performed at 220°C . It indicated that the steady state CO_2 conversions were ranged between 11.78 to 26.12% with corresponding to the reaction rate at 6.30 to $14.35 \times 10^2 \text{ g CH}_2/\text{g cat.h}$ of cobalt supported on spherical silica and alumina-silica composites supported catalysts. It was found that at the reaction conditions used, the use of CoAlSSP1000 (1:3) exhibited a much higher CO_2 hydrogenation conversion and CH_4 selectivity than all other catalysts in this study. On the other hand, for used of CoAlSSP1000 (1:1) resulted in lowest activity and selectivity. It was found that the alumina significantly enhanced the activity and selectivity to methane of CO_2 hydrogenation, indicating the balance among dispersion of alumina, reduction degree of silica and BET surface area in term of pore size can be facilitate [Sun et al., 2010]. The rate vs. time on stream of cobalt supported on spherical silica and alumina-silica composites supported catalysts with reaction temperature at 220°C is illustrated in Figure 5.19.

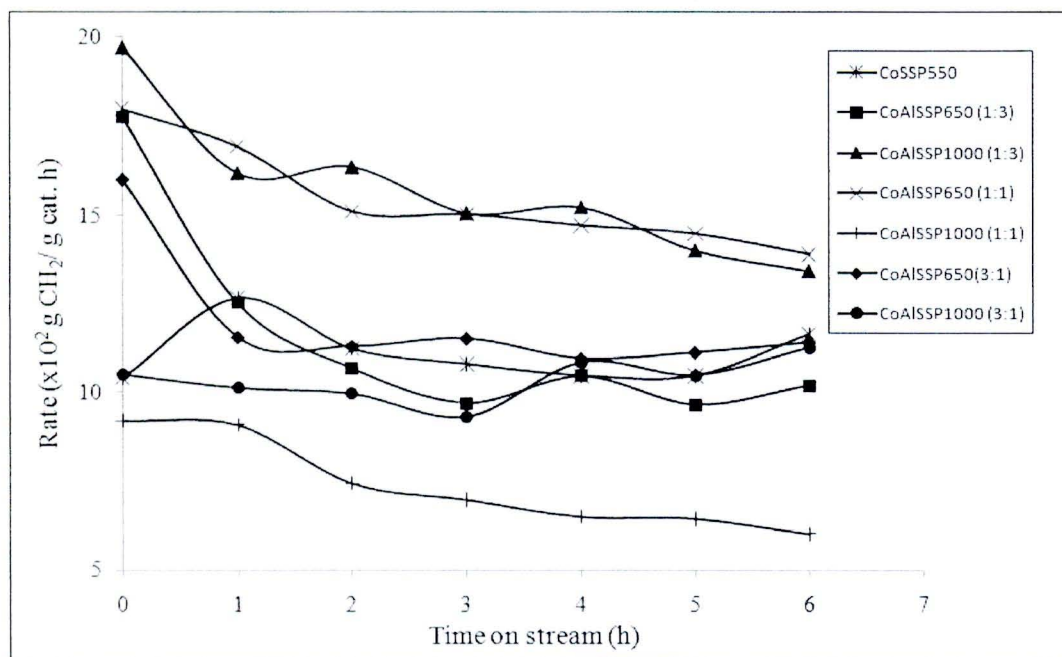


Figure 5.19 Reaction rate at 220°C vs. time on stream of silica and alumina-silica composites supported cobalt catalysts.